



Primary lymphomas of the female genital tract: imaging findings

Mónica Alexandra Alves Vieira, Teresa Margarida Cunha

ABSTRACT

Primary lymphomas of the female genital tract are extremely rare, and a definitive diagnosis requires correlation of the clinical, radiological, and pathological findings. Unlike non-lymphomatous malignant tumors, the treatment of lymphoma is typically nonsurgical, thus raising the possibility of lymphoma in the differential diagnosis of a pelvic mass, a radiologist can significantly change the approach to the disease. Although some imaging findings may appear nonspecific, others may suggest the possibility of lymphoma, such as the presence of one or more solid, well-defined, homogeneous masses without necrosis despite a large size or the presence of diffuse infiltration leading to organomegaly with architectural preservation. Additionally, pelvic lymphadenopathy may be evident. In this pictorial essay, we discuss the radiological appearances of gynecological primary lymphomas, grouped by organ, in ultrasonography, computed tomography, and magnetic resonance imaging.

Lymphomas of the female genital tract are uncommon. Most of them are secondary tumors (primary tumors are very rare), with a few case reports in the literature. Lymphomas can be classified as non-Hodgkin lymphoma (NHL) and Hodgkin lymphoma (HL), which show different imaging patterns. In contrast to Hodgkin lymphoma, extranodal involvement is more frequent in non-Hodgkin lymphoma as well as dissemination to noncontiguous nodes with involvement of different nodal groups (1, 2). Extranodal lymphoma is classified as primary or secondary. Primary lymphoma refers to the following: 1) lymphomatous involvement confined to a solitary extranodal site and its immediately adjacent lymph node group or contiguous structures at the time of diagnosis; 2) the absence of abnormal cells in the peripheral blood and bone marrow; and 3) the absence of further lymphomatous lesions at remote sites after several months (3).

Clinical staging is based on a combination of clinical, radiologic, and surgical findings, following the Ann Arbor staging system (Table) (4). Currently recommended approaches for staging consist of routine physical examination, laboratory analysis, chest X-ray, cross-sectional imaging of the chest, abdomen, and pelvis, bone marrow biopsy, and lumbar puncture (in selected cases of NHL) for any stage beyond clinical stage IA. Fluorine-18 fluorodeoxyglucose positron emission tomography (^{18}F -FDG PET) is included in the most recent recommendations for pre-treatment evaluation, particularly in the setting of equivocal results (4).

The presenting symptoms of primary lymphomas of the female genital tract depend on the site involved and the aggressiveness of the tumor. These include vaginal bleeding, vaginal discharge, an abdominal mass, dyspareunia, perineal discomfort, urinary retention, or constitutional symptoms (5–7). The prognosis varies according to the stage and histological subtype (4).

Imaging techniques

A definitive diagnosis requires a biopsy (bone marrow, lymph node, or mass), but imaging plays an important role in the noninvasive management of lymphomas, including the establishment of a provisional diagnosis, staging of disease, and follow-up. Complications of both the disease and treatment may be also recognized.

Ultrasonography (US) can be useful in the initial investigation of primary lymphomas of the female genital tract, but computed tomography (CT) and magnetic resonance imaging (MRI) are better for assessing the lesion size, structure, and extension to adjacent structures. MRI also provides greater accuracy in the characterization of pelvic tumors. The role of lymphangiography has been superseded by these techniques (1, 8).

From the Department of Radiology (M.A.A.V. ✉ moni.a.a.vieira@gmail.com), Hospital José Joaquim Fernandes-Unidade Local de Saúde do Baixo Alentejo, Beja, Portugal; the Department of Radiology (T.M.C.), Instituto Português de Oncologia de Lisboa Francisco Gentil, Lisbon, Portugal.

Received 11 July 2013; revision requested 8 August 2013; revision received 30 August 2013; accepted 16 September 2013.

Published online 10 January 2014.
DOI 10.5152/dir.2013.13288

Gallium-67 (⁶⁷Ga) scintigraphy, ¹⁸F-FDG PET, and PET-CT are valuable for the identification of disease in normal-sized organs, the differentiation of post-treatment fibrosis and residual viable tumor, detection of early recurrence, prediction of an early response to chemotherapy, and determination of prognosis (2, 9). Advantages of PET over ⁶⁷Ga scintigraphy are higher accuracy, better spatial resolution, same day imaging, and a lower radiation dose (2).

The selection of appropriate imaging modalities is complex and depends on the patient, radiologist, and institutional constraints.

Imaging features

Generally, the pattern of lymphomatous involvement may be nodular, multinodular, or diffuse. Regarding the first two disease patterns, solid, round, well-defined, homogeneous lesions are present with a minimal mass effect for their size. Necrosis, hemorrhage, and calcification are rare in the absence of treatment. In diffuse disease, there is uniform infiltration of the parenchyma, producing organomegaly without structural abnormalities. In the latter case, the organ contour usually is normal or slightly abnormal, even in advanced disease (2, 3, 6, 7, 10). Pelvic lymphadenopathy may also be evident (5).

In the reported cases, on US, lym-

phomas tend to appear hypoechoic, with an absence of posterior acoustic enhancement and showing mild vascularization on color Doppler US. On CT, lymphomas show a density similar to that of muscle or moderated hypoattenuation when compared with the surrounding parenchyma, but usually have attenuation values higher than water. On MRI, lymphomas usually exhibit low-to-intermediate signal intensity on T1-weighted imaging and moderately high signal intensity on T2-weighted imaging (2, 3, 6, 7, 10, 11).

Enhancement after the administration of intravenous contrast material tends to be mild and uniform. However, in some cases, contrast-enhanced images may depict subtle heterogeneous areas that are not visible on unenhanced images. Rarely, central necrosis and hemorrhage may produce a heterogeneous appearance on unenhanced or contrast-enhanced images (2, 6, 7, 10, 12).

On PET, a standardized uptake value greater than 2.5 suggests malignancy (5).

Ovarian lymphomas

The age range of patients diagnosed with ovarian lymphoma is from 18 months to 74 years (5).

Unilateral and bilateral ovarian involvement shows a similar incidence (5). The lesions are frequently larger,

and ascites is infrequent (12). Peritoneal involvement is evident in less than half of cases (5). Extraovarian extension occurs most commonly through the pelvic and para-aortic lymph nodes (5).

The presence of septal structures showing hyperintensity on T2-weighted imaging, and a linear arrangement of small cysts at the periphery of tumor was reported (Fig. 1) (11).

The differential diagnosis of ovarian primary lymphoma is usually made with ovarian epithelial neoplasms (which normally have a complex structure with cystic/necrotic areas and solid components with early enhancement), sarcomas (which are less likely to be bilateral), and other predominantly solid ovarian tumors such as fibromas, thecomas, and Brenner cell tumors that have low growth rates. Additionally, in children, germ cell tumors and neuroblastomas usually have an inhomogeneous structure. Metastases should be considered if a primary lesion or other sites of metastases are observed (3). A concurrent finding of adenopathy can help the diagnosis.

Lymphomas of the uterus body and cervix

The median age at diagnosis is in the fourth to fifth decades (5, 7). Most primary uterine lymphomas arise from the cervix; however, in most cases, both the

Table. Ann Arbor system for staging of lymphoma (4)

Stage	Description
I	Involvement of a single lymph node region or lymphoid structure (e.g., the spleen, thymus, Waldeyer's ring) or involvement of a single extralymphatic site (IE)
II	Involvement of more than one lymphatic region on only one side of the diaphragm
IIE	Localized involvement of one extralymphatic organ or site and its regional lymph nodes with or without other nodes on the same side of the diaphragm
IIS	Involvement of more than one lymphatic region on only one side of the diaphragm plus involvement of the spleen
IIES	Both
III	Involvement of lymph node regions on both sides of the diaphragm
IIIE	Involvement of lymph node regions on both sides of the diaphragm plus localized involvement of an extra lymphatic organ or site
IIIS	Involvement of lymph node regions on both sides of the diaphragm plus involvement of the spleen
IIIES	Both
IV	Diffuse or disseminated involvement of one or more extralymphatic organs or tissues with or without associated lymph node enlargement. Organs considered distant include the liver, bone, bone marrow, lung and/or pleura, and kidney

Suffices to each stage:

A, without symptoms—e.g., stage IA or IIIA.

B, with symptoms (night sweats, unexplained fever >38°C, and unexplained weight loss >10% within the last six months)—e.g., stage IIB or IVB.

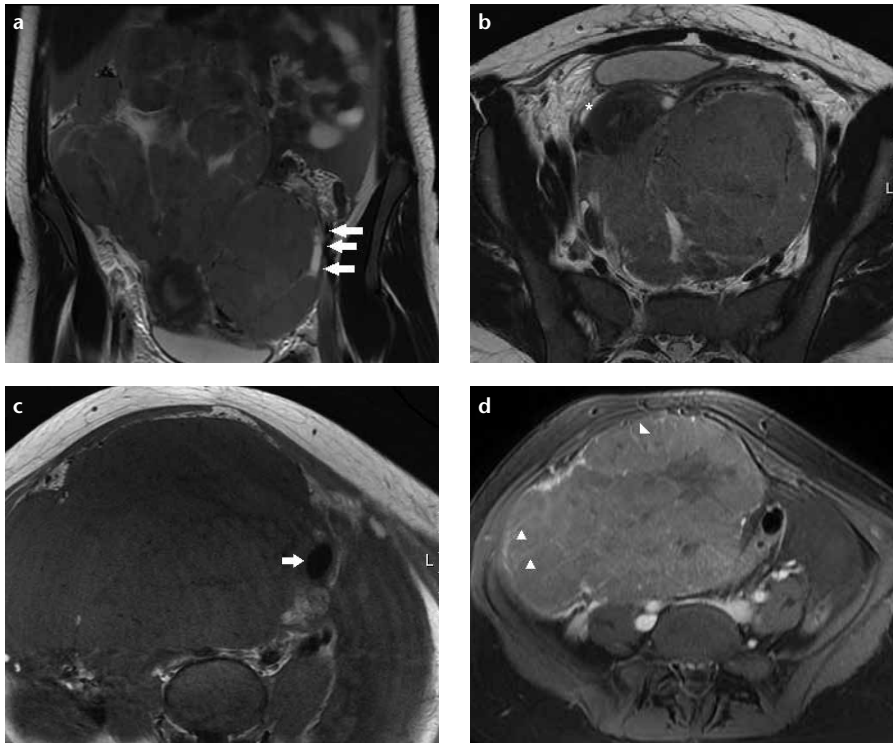


Figure 1. a–d. A 23-year-old female with bilateral primary B-cell non-Hodgkin lymphoma of the ovaries. The patient was human immunodeficiency virus positive and presented with an abdominal mass. Coronal (a) and axial (b) fast spin-echo T2-weighted MRI showed a solid, lobulated, large, bilateral adnexal mass with intermediate signal intensity and hyperintense septal structures, some small cysts with smooth walls, consistent with follicles at the periphery of the tumor (a, arrows). Only a small amount of ascites was observed (b, asterisk). On axial spin-echo T1-weighted MRI (c), the tumor demonstrated low signal intensity, and a follicle was observed (arrow). On axial contrast-enhanced fat-saturated T1-weighted MRI (d), the septa showed marked enhancement (arrowheads) compared with the slight enhancement observed in the other solid portion.

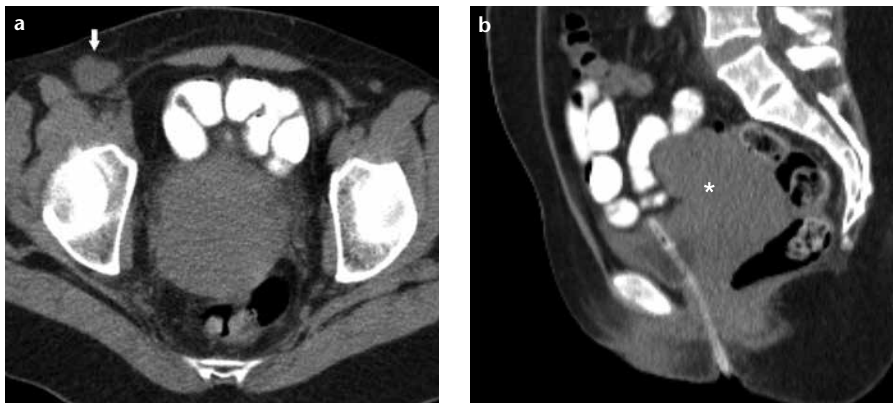


Figure 2. a, b. A 47-year-old female with primary lymphoma of the uterine body and cervix. The patient presented with hydronephrosis on routine US, and a pelvic mass was noted at physical examination. Axial (a) and sagittal (b) unenhanced CT of the pelvis and abdomen denoted a diffuse, homogeneous enlargement of the uterine body and cervix (asterisk) that did not show a cleavage plane with the bladder. Additionally, pelvic lymphadenopathy was observed in the right external iliac and inguinal chains (a, arrow). A biopsy of the cervix revealed diffuse, large B-cell non-Hodgkin lymphoma.

cervix and uterine body are involved (5). Symmetrical diffuse uterine enlargement is the most common appearance (Fig. 2), but it may seem as a large lobulated mass or as multiples nodules.

These lesions have also been described as a submucosal mass mimicking a leiomyoma. Usually, the endometrium and cervical epithelium are not involved (7). Bladder and vaginal invasion may

be seen (Fig. 3) (6, 7). Significant enhancement with gadolinium was reported, a finding that is slightly unusual compared with lymphoma in solid abdominal organs (2).

The differential diagnosis includes cervical carcinoma, small-cell carcinoma of the uterus, metastases, and sarcoma (5). Architectural preservation and sparing of the uterine junctional and inner layer of the cervical stroma, despite the extensive involvement of the uterine body, may suggest the diagnosis of lymphoma (6). In cases affecting the mucosa, it is difficult to differentiate lymphoma from the much more common epithelial neoplasms. In these cases, the presence of a relatively homogeneous tumor, despite the larger tumor size, may be helpful for diagnosis. Apparent septations postintra-venous contrast enhancement, leading to a nodular appearance, was suggested as another evocative finding (7).

Lymphomas of the vagina

The mean age at diagnosis is 50 years (5). The tumor may be infiltrative or lobular (Fig. 4). The infiltrative form is more common and appears as diffuse thickening of the vaginal wall (Fig. 5) (10). Contiguous spread of the tumor into the cervix may be observed (10).

The differential diagnosis of primary lymphoma of the vagina is made with other more common vaginal neoplasms, such as carcinoma. An intact mucosa is distinctive of lymphoma (10).

Lymphomas of the endometrium

Primary endometrial lymphoma is particularly rare and may appear as diffuse thickening of the endometrium without myometrial involvement or as a polypoid lesion with or without a diffuse coating of the endometrium (Fig. 6) (13). Endometrial hyperplasia, endometrial polyps, and carcinoma can have similar morphologic aspects and must be considered in the differential diagnosis.

Lymphomas of the fallopian tubes

Only rare cases of primary tubal lymphoma have been reported; most cases of fallopian tube involvement reflect more extensive disease arising in the ovary. No study has described in detail the imaging findings.

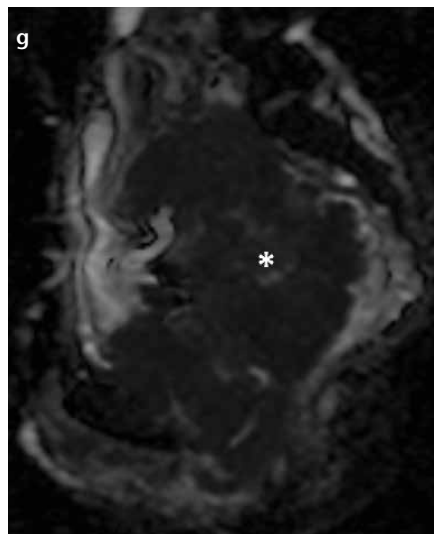
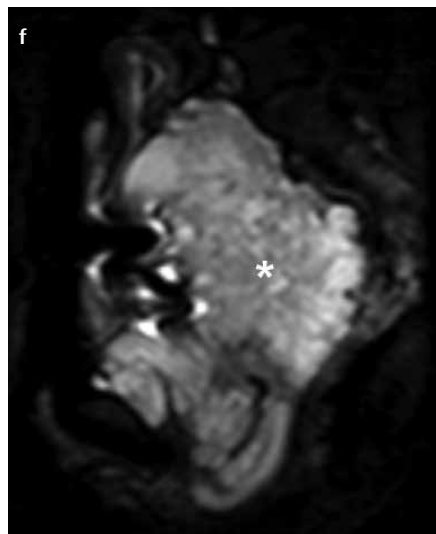
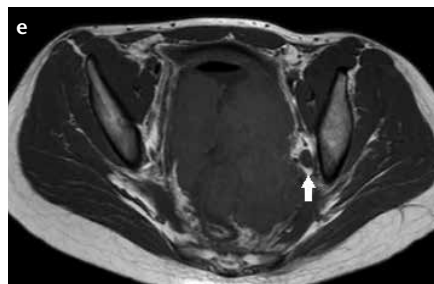
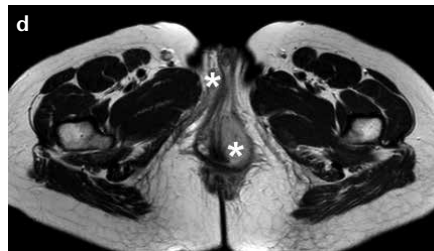
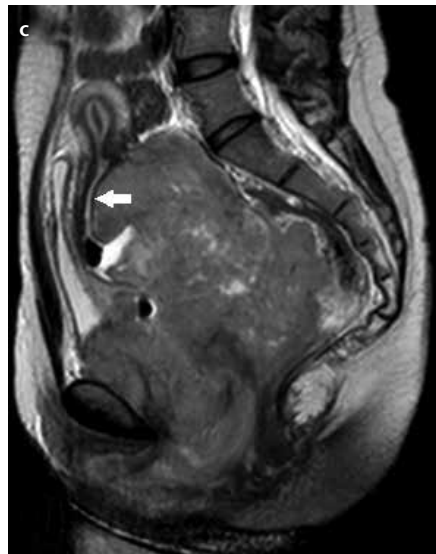
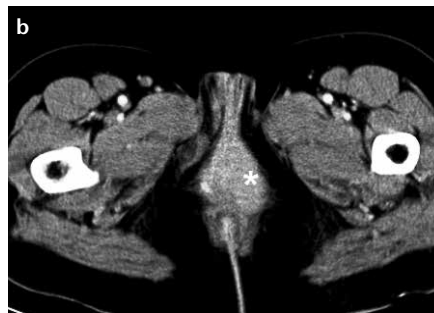


Figure 3. a–g. A 25-year-old female with primary lymphoma of the cervix and vagina. The patient had a history of genital human papilloma virus infection and presented with vaginal bleeding and a vaginal fetid discharge. Axial contrast-enhanced CT of the pelvis (a, b) showed a homogeneous, lobulated mass of the vagina with uniform enhancement that invaded the posterior pelvic wall (a, white arrow) and vulva (b, asterisk). Pelvic lymphadenopathy was observed in the left external obturator chain (a, black arrow). Sagittal fast spin-echo T2-weighted MRI (c) showed a moderately hyperintense lobulated tumor involving the vaginal wall and uterine cervix (arrow) and extending down into the perineum. Although the mass was very large, the cervical epithelium remained as a hyperintense band anteriorly to the tumor (c, arrow). Axial fast spin-echo T2-weighted MRI (d) showed invasion of the vulva (asterisks). Axial spin-echo T1-weighted MRI (e) showed that the tumor had low signal intensity and that pelvic lymphadenopathy was evident (arrow). Sagittal diffusion-weighted images (f, g) acquired at a b value of 600 s/mm² demonstrated high signal intensity of the mass (f, asterisk) and a low apparent diffusion coefficient on a corresponding apparent diffusion coefficient map (g, asterisk). A biopsy of the tumor revealed diffuse large B-cell non-Hodgkin lymphoma.

Figure 4. A 64-year-old female with primary lymphoma of the vagina. The patient presented with vaginal bleeding. Axial unenhanced CT of the pelvis showed a solid, well-defined, homogeneous, isodense mass of the vagina (asterisk). A biopsy of the vagina revealed B-cell non-Hodgkin lymphoma.

The age of presentation is in the third to fifth decades (14, 15). Lymphomatous involvement may be unilateral or bilateral (14, 15), having been associated with chronic inflammation (tubo-ovarian abscess or endometriosis) in some cases (15). In some reported cases, the patients presented with a complex pelvic mass; in other cases, lymphoma was found as an incidental finding during pelvic surgery (14, 15).

A differential diagnosis includes inflammatory pelvic disease, carcinoma, and metastases (15).

Residual disease

A commonly encountered problem on follow-up is distinguishing between fibrosis/residual nonviable tissue after therapy and residual disease.

In MRI, reducing the signal intensity on T2-weighted imaging is associated with reducing the cellular density and successful treatment (10). Fibrotic tissue produces very low signal intensity on T2-weighted imaging and no enhancement with gadolinium. In the early stages of fibrosis and in inflammatory changes induced by radiotherapy, the signal intensity on T2-weighted imaging may be intermediate or high, but shows absence of restriction on (low signal intensity) diffusion-weighted images.

¹⁸F-FDG PET can also detect very small foci of disease in residual masses (2), but inflammatory changes from recent surgery and radiation therapy have also demonstrated increased ¹⁸F-FDG uptake (9).



Figure 5. a–c. A 32-year-old female with primary lymphoma of the vagina. The patient presented with vaginal bleeding. Sagittal fast spin-echo T2-weighted MRI (a) showed a slightly hyperintense infiltrating tumor, resulting in a diffuse thickening of the vaginal wall extending to cervix. Note the presence of intact mucosa (arrow). A submucosal fibroid was also observed in the mid-uterine body. On axial spin-echo T1-weighted MRI (b), the tumor showed low signal intensity. On sagittal contrast-enhanced fat-saturated T1-weighted MRI (c), the tumor showed uniform enhancement. No enlarged locoregional lymph nodes were identified. A biopsy of the vagina revealed diffuse large B-cell non-Hodgkin lymphoma, and a biopsy of the cervix was negative.

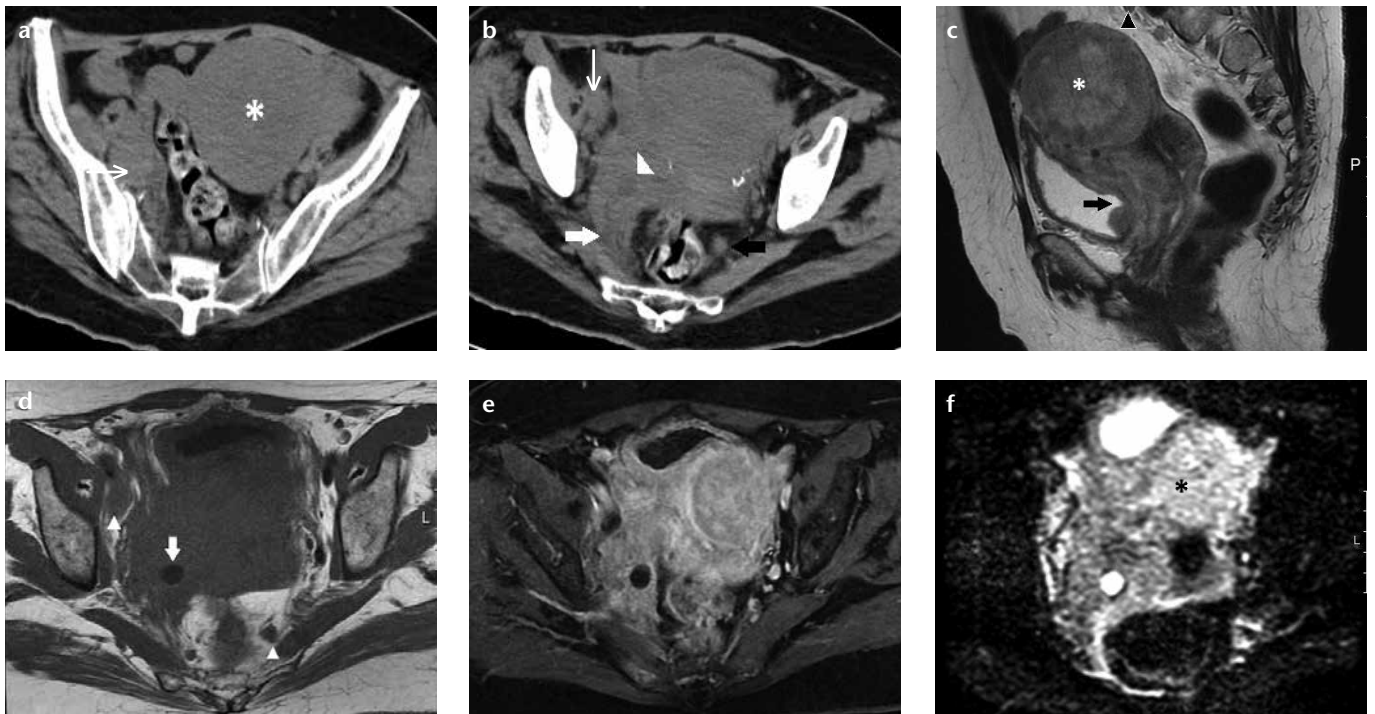


Figure 6. a–f. A 71-year-old female with primary lymphoma of the endometrium. She presented with vaginal bleeding and a pelvic mass. Axial unenhanced CT of the pelvis (a, b) showed homogeneous enlargement of the uterine body (a, asterisk) and a pelvic isodense mass extending to the parametrium, invading the posterior pelvic wall (b, thick arrow), encasing the pelvic ureter (b, arrowhead) and causing hydronephrosis. Enlarged locoregional lymph nodes were identified (a, b, thin arrows). Sagittal fast spin-echo T2-weighted (c) MRI showed a moderately hyperintense polypoid tumor of the endometrium (asterisk), extending anteriorly and inferiorly and involving the myometrium, cervix, anterior vaginal wall, and bladder wall (arrow). The cervical epithelium was spared. Axial spin-echo T1-weighted MRI (d) showed that the tumor had intermediate signal intensity with an enlarged pelvic ureter showing low signal intensity (arrow). Enlarged locoregional lymph nodes are shown (arrowheads). On axial contrast-enhanced fat-saturated T1-weighted MRI (e), the tumor showed uniform mild enhancement. Axial diffusion-weighted images acquired at a b value of 600 s/mm² (f) showed high signal intensity of the mass (asterisk). A biopsy of the tumor revealed diffuse non-Hodgkin lymphoma.

Conclusion

Lymphoma is a diagnostic challenge, particularly in the context of a newly discovered pelvic mass. Despite the absence of specific imaging

patterns, there are radiologic appearances that must alert the radiologist about the possibility of primary lymphomas of the female genital tract. Familiarity with these appearances

may allow the radiologist to offer an accurate differential diagnosis, avoiding unnecessary surgical interventions and the associated morbidity and mortality.

Conflict of interest disclosure

The authors declared no conflicts of interest.

References

1. Leite NP, Kased N, Hanna RF, et al. Cross-sectional imaging of extranodal involvement in abdominopelvic lymphoproliferative malignancies. *Radiographics* 2007; 27:1613–1634. [\[CrossRef\]](#)
2. Halliday T, Baxter G. Lymphoma: pictorial review. II. *Eur Radiol* 2003; 13:1224–1234.
3. Crawshaw J, Sohaib SA, Wotherspoon A, Shepherd JH. Primary non-Hodgkin's lymphoma of the ovaries: imaging findings. *Br J Radiol* 2007; 80:155–158. [\[CrossRef\]](#)
4. Matasar MJ, Zelenetz AD. Overview of lymphoma diagnosis and management. *Radiol Clin North Am* 2008; 46:175–198. [\[CrossRef\]](#)
5. Taheri MR, Dighe MK, Kolokythas O, True LD, Bush WH. Multifaceted genitourinary lymphoma. *Curr Probl Diagn Radiol* 2008; 37:80–93. [\[CrossRef\]](#)
6. Marin C, Seoane JM, Sanchez M, Ruiz Y, Garcia JA. Magnetic resonance imaging of primary lymphoma of the cervix. *Eur Radiol* 2002; 12:1541–1545. [\[CrossRef\]](#)
7. Goto N, Oishi-Tanaka Y, Tsunoda H, Yoshikawa H, Minami M. Magnetic resonance findings of primary uterine malignant lymphoma. *Magn Reson Med Sci* 2007; 6:7–13. [\[CrossRef\]](#)
8. Chua SC, Rozalli FI, O'Connor SR. Imaging features of primary extranodal lymphomas. *Clin Radiol* 2009; 64:574–588. [\[CrossRef\]](#)
9. Subhas N, Patel PV, Pannu HK, Jacene HA, Fishman EK, Wahl RL. Imaging of pelvic malignancies with in-line FDG PET-CT: case examples and common pitfalls of FDG PET. *Radiographics* 2005; 25:1031–1043. [\[CrossRef\]](#)
10. Jenkins N, Husband J, Sellars N, Gore M. MRI in primary non-Hodgkin's lymphoma of the vagina associated with a uterine congenital anomaly. *Br J Radiol* 1997; 70:219–222.
11. Mitsumori A, Joja I, Hiraki Y. MR appearance of non-Hodgkin's lymphoma of the ovary. *AJR Am J Roentgenol* 1999; 173:245. [\[CrossRef\]](#)
12. Ferrozzi F, Catanese C, Uccelli M, Bassi P. Ovarian lymphoma. Findings with ultrasonography, computerized tomography and magnetic resonance. *Radiol Med* 1998; 95:493–497.
13. Lemos S, Magalhães E, Sousa V, Dias M, de Oliveira C. Primary endometrial B-cell lymphoma: case report. *Eur J Gynaecol Oncol* 2008; 29:656–658.
14. Gaffan J, Herbertson R, Davis P, Dogan A, Jones A. Bilateral peripheral T-cell lymphoma of the fallopian tubes. *Gynecol Oncol* 2004; 95:736–738. [\[CrossRef\]](#)
15. Alduaij A, Hansen K, Zhang C. Primary follicular lymphoma of the fallopian tube found incidentally in a patient treated for endometrial carcinoma: a case report. *Diagn Pathol* 2010; 5:44. [\[CrossRef\]](#)